Nitric oxide stimulates type IV MSHA pilus retraction in *Vibrio cholerae* via activation of the phosphodiesterase CdpA

Hannah Q. Hughes[a], Kyle A. Floyd[b], Sajjad Hossain[c], Sweta Anantharaman[c], David T. Kysela[d], Mikls Zöldi[e], László Barna[e], Yuanchen Yu[f], Michael P. Kappler[f], Triana N. Dalia[a], Ram C. Podicheti[g], Douglas B. Rusch[g], Meng Zhuang[h], Cassandra L. Fraser[h], Yves V. Brun[d], Stephen C. Jacobson[f], James B. McKinlay[a], Fitnat H. Yildiz[b], Elizabeth M. Boon[c,i], and Ankur B. Dalia[a,1]

[a]Department of Biology, Indiana University, Bloomington, IN 47405; [b]Department of Microbiology and Environmental Toxicology, University of California, Santa Cruz, CA 95064; [c]Department of Chemistry, Stony Brook University, Stony Brook, NY 11794; [d]Department of Microbiology, Infectious Diseases, and Immunology, Université de Montréal, Montréal, QC H3T 1J4, Canada; [e]Department of Psychological and Brain Sciences, Indiana University, Bloomington, IN 47405; [f]Department of Chemistry, Indiana University, Bloomington, IN 47405; [g]Center for Genomics and Bioinformatics, Indiana University, Bloomington, IN 47405; [h]Department of Chemistry, University of Virginia, Charlottesville, VA 22904; and [i]Institute of Chemical Biology & Drug Discovery, Stony Brook University, Stony Brook, NY 11794

Edited by Bonnie Bassler, Department of Molecular Biology, Princeton University, Princeton, NJ; received May 3, 2021; accepted December 21, 2021

Bacteria use surface appendages called type IV pili to perform diverse activities including DNA uptake, twitching motility, and attachment to surfaces. The dynamic extension and retraction of pili are often required for these activities, but the stimuli that regulate these dynamics remain poorly characterized. To address this question, we study the bacterial pathogen *Vibrio cholerae*, which uses mannose-sensitive hemagglutinin (MSHA) pili to attach to surfaces in aquatic environments as the first step in biofilm formation. Here, we use a combination of genetic and cell biological approaches to describe a regulatory pathway that allows *V. cholerae* to rapidly abort biofilm formation. Specifically, we show that *V. cholerae* cells retract MSHA pili and detach from a surface in a diffusion-limited, enclosed environment. This response is dependent on the phosphodiesterase CdpA, which decreases intracellular levels of cyclic-di-GMP to induce MSHA pilus retraction. CdpA contains a putative nitric oxide (NO)–sensing NosP domain, and we demonstrate that NO is necessary and sufficient to stimulate CdpA-dependent detachment. Thus, we hypothesize that the endogenous production of NO (or an NO-like molecule) in *V. cholerae* stimulates the retraction of MSHA pili. These results extend our understanding of how environmental cues can be integrated into the complex regulatory pathways that control pilus dynamic activity and attachment in bacterial species.

type IV pili | biofilm | attachment

Type IV pili (T4P) are nearly ubiquitous nanomachines in bacteria (1). These structures promote a wide variety of functions, including the uptake of DNA for horizontal gene transfer (2), motility on surfaces (3), and attachment to surfaces (4–6). Pili are filaments composed of a single repeating protein called the major pilin (7). Major pilin subunits are dynamically assembled into a helical filament on an inner membrane platform protein through the action of a specific motor ATPase protein. This dynamic process of assembly promotes the extension of the pilus filament from the cell surface. Conversely, through the action of an antagonistic ATPase, pilus filaments are depolymerized and major pilin subunits are recycled into the membrane. The dynamic process of pilus disassembly results in the retraction of these structures (8–10). The dynamic extension and retraction of pili are crucial for their diverse functions. In particular, this dynamic activity represents one important mechanism that bacteria use to interact with and respond to their environments. However, the mechanisms by which bacteria regulate pilus dynamic activity in response to environmental cues remain poorly characterized. To address this, we examined the pilus dynamic activity of the *Vibrio cholerae* type IV mannose-sensitive hemagglutinin (MSHA) pilus system. MSHA pili are expressed when *V. cholerae* inhabits its aquatic reservoir and are critical for its attachment to abiotic surfaces (11–13). Here, we uncover an environmental condition that stimulates pilus retraction, and we characterize the molecular mechanism underlying this response.

Results

MSHA Pilus Retraction Is Required for Cell Detachment from Well Slides. MSHA pili are critical for attachment to abiotic surfaces (12, 13) (*SI Appendix*, Fig. S1*A*), and labeling of MSHA pili (5) (*SI Appendix*, Fig. S1*B*) reveals that pilus retraction can promote cell detachment (14) (Fig. 1*A* and Movie S1). The physiological cues that regulate pilus dynamic activity in most T4P to influence their downstream functions, however, remain unclear. One condition we identified that induces cell detachment in *V. cholerae* is the incubation of cells in the well of a glass slide. We found that cells progressively detach in a wave that propagates from the center of the well to the edge, leaving only cells on the periphery of the well attached to the surface (Fig. 1*B*).

Significance

All organisms sense and respond to their environments. One way bacteria interact with their surroundings is by dynamically extending and retracting filamentous appendages from their surface called pili. While pili are critical for many functions, such as attachment, motility, and DNA uptake, the factors that regulate their dynamic activity are poorly understood. Here, we describe how an environmental signal induces a signaling pathway to promote the retraction of mannose-sensitive hemagglutinin pili in *Vibrio cholerae*. The retraction of these pili promotes the detachment of *V. cholerae* from a surface and may provide a means by which *V. cholerae* can respond to changes in its environment.

Author contributions: H.Q.H., K.A.F., D.T.K., Y.V.B., S.C.J., F.H.Y., E.M.B., and A.B.D. designed research; H.Q.H., K.A.F., S.H., S.A., D.T.K., M. Zöldi, L.B., T.N.D., and R.C.P. performed research; Y.Y., M.P.K., M. Zhuang, C.L.F., S.C.J., and J.B.M. contributed new reagents/analytic tools; H.Q.H., D.B.R., J.B.M., F.H.Y., E.M.B., and A.B.D. analyzed data; and H.Q.H. and A.B.D. wrote the paper.

The authors declare no competing interest.

This article is a PNAS Direct Submission.

[1]To whom correspondence may be addressed. Email: ankdalia@indiana.edu.

This article contains supporting information online at http://www.pnas.org/lookup/suppl/doi:10.1073/pnas.2108349119/-/DCSupplemental.

Published February 8, 2022.

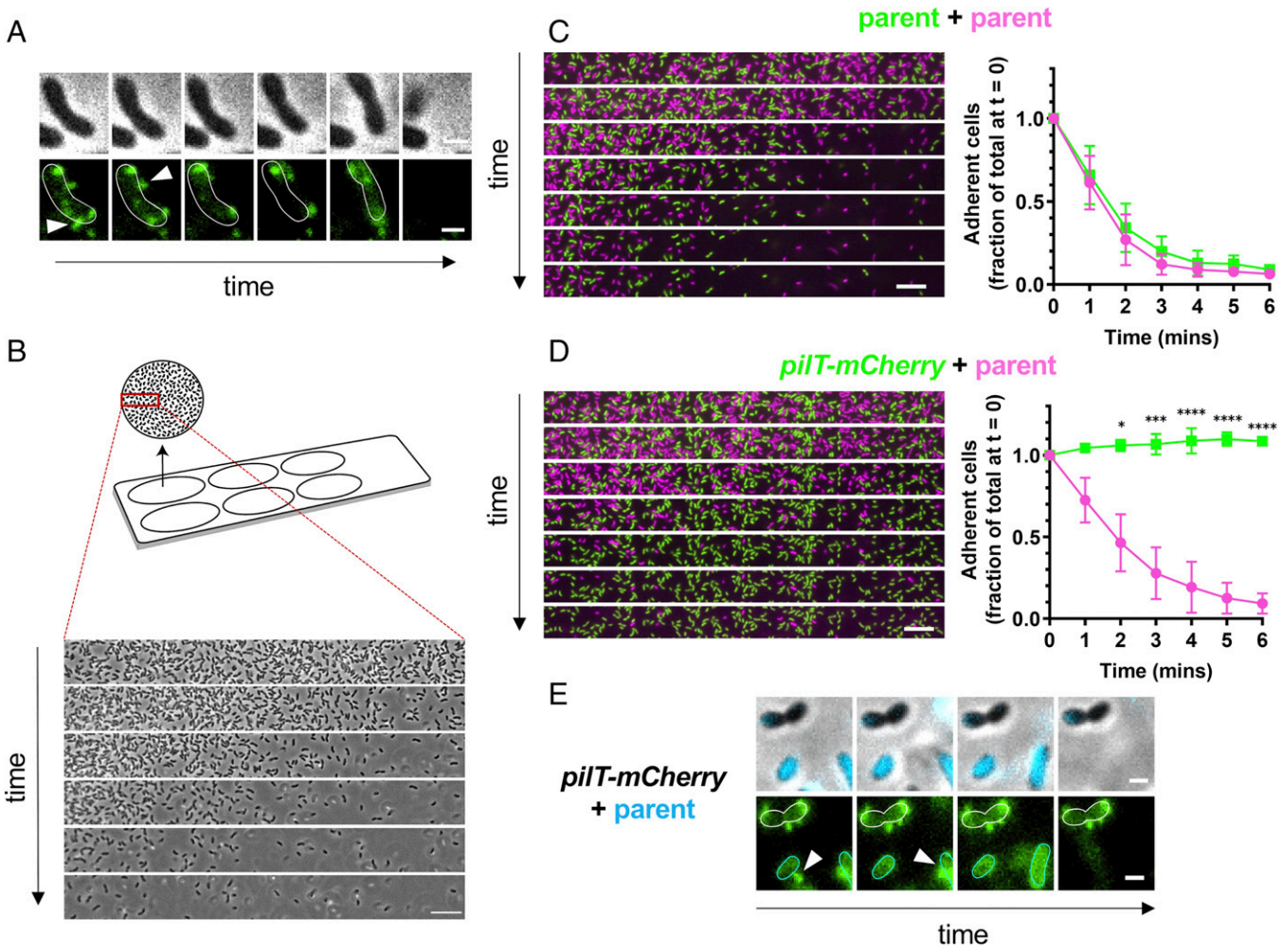

Fig. 1. Cells rapidly detach from the surface of a glass well slide in a manner that is dependent on MSHA pilus retraction. (*A*) Representative montage illustrating that MSHA pilus retraction precedes cell detachment (Movie S1). Phase images (*Top*) show cell boundaries, and FITC channel (*Bottom*) images show AF488-mal labeled MSHA pili. White arrows indicate examples where pili retract prior to cell detachment. There are 10-s intervals between frames. Scale bar, 1 μm. (*B*) Diagram of experimental setup to observe cell detachment in a glass well slide (*Top*). Representative phase contrast images (*Bottom*) of cell detachment over time. There is a 1-min interval between frames. Scale bar, 10 μm. (*C* and *D*) MixD assays of the indicated strains. Cells expressed GFP (green) or mCherry (fuchsia) as indicated by the color-coded genotypes. Representative montages show time-lapse imaging (*Left*) with 1-min intervals between frames (Movies S2 and S3). Scale bar, 10 μm. The quantification of three biological replicates is shown in the line graph (*Right*) and is displayed as the mean ± SD. Statistical comparisons were made by one-way ANOVA and post hoc Holm-Sídák test. $*P < 0.05$, $***P < 0.001$, $****P < 0.0001$. (*E*) Representative montage shows the labeled fluorescent MSHA pili in a mixture of a *pilT-mCherry* strain and a CyPet-expressing parent strain (Movie S4). Phase contrast images with overlaid CyPet fluorescence in cyan (*Top*) distinguish the two strains, and FITC fluorescence images in green (*Bottom*) show AF488-mal labeled pili. Parent cells are outlined in cyan and *pilT-mCherry* cells are outlined in white. There are 20-s intervals between frames. Scale bar, 1μm. The PilT-mCherry construct does not exhibit detectable mCherry fluorescence in *D* and *E*.

To further characterize this response, we developed an assay that allowed us to simultaneously evaluate the detachment of multiple strains in a consistent environment. This assay, henceforth called a mixed detachment (MixD) assay, involves mixing equal proportions of two strains that express distinct fluorescent markers and subsequently tracking the detachment of each strain via simple epifluorescence time-lapse microscopy. To validate this approach, we performed a MixD assay of two parent strains expressing either green fluorescent protein (GFP) or mCherry (Fig. 1*C* and Movie S2). As expected, the two parent strains detached at similar rates over the course of ∼4 min. Importantly, this assay facilitates the direct comparison of the detachment kinetics of mutants with the parent strain under identical environmental conditions. Therefore, we employed MixD assays to identify factors that regulate this detachment response.

Because MSHA pilus retraction can promote cell detachment (14) (Fig. 1*A*), we first wanted to determine if retraction was required for this detachment response. Deletion of the retraction motor gene *pilT* is a commonly employed approach for preventing pilus retraction, which results in hyperpiliation of other T4P (15, 16). For MSHA pili, however, deletion of *pilT* results in a dramatic reduction in the number of pili present on the surface (14, 17) (*SI Appendix*, Fig. S2 *A* and *B*), for reasons that remain unclear. As an alternative, we took advantage of a natively expressed PilT-mCherry fusion, which we have serendipitously found reduces PilT activity without affecting MSHA piliation (*SI Appendix*, Fig. S2 *A–D*). We performed a MixD assay of the parent and PilT-mCherry strains and found that while the parent strain detached, the PilT-mCherry strain remained attached throughout the time-lapse (Fig. 1*D* and Movie S3). We further verified that when the parent strain detaches, it is preceded by the retraction of the MSHA pilus, and the PilT-mCherry cells that remain attached retain extended MSHA pili (Fig. 1*E* and Movie S4), consistent with

a lack of retraction in the latter strain background. This observation indicates that MSHA pilus retraction is required for detachment under these conditions.

MSHA Pilus Retraction and Cell Detachment Are Dependent on Allosteric Regulation of MshE Activity by c-di-GMP. Transitions between sessile and motile lifestyles are often mediated by the secondary messenger cyclic-di-GMP (c-di-GMP) (18). Indeed, c-di-GMP regulates *V. cholerae* motility and biofilm formation in part through the control of MSHA dynamic activity (14, 19). Specifically, when c-di-GMP levels are elevated through the action of diguanylate cyclases (DGCs), c-di-GMP can bind to the extension motor MshE and allosterically induce pilus extension (20). Correspondingly, decreased levels of c-di-GMP, which may occur via the action of EAL- or HD-GYP-domain-containing phosphodiesterases (PDEs) that cleave c-di-GMP, reduce MshE activity (14, 20) and prevent cell attachment. Thus, we hypothesized that the detachment phenomenon on slides may be caused by a reduction in intracellular c-di-GMP. If so, we would predict that elevating intracellular c-di-GMP should prevent or delay detachment. To test this, we generated strains where we could ectopically express a DGC, *dcpA* (21), to elevate intracellular c-di-GMP levels (P_{BAD}-*dcpA*). Elevated c-di-GMP can also induce the expression of the *vps* and *rbm* loci (22), which encode *Vibrio* polysaccharide and biofilm matrix proteins that can confound attachment in these experiments. Therefore, we deleted both loci (ΔVC0917-VC0939; here called Δ*vps*) in the P_{BAD}-*dcpA* background to ensure that attachment in these assays was due to MSHA pili (*SI Appendix*, Fig. S1 *C* and *D*). When tested in a MixD assay, we found that upon induction of *dcpA*, P_{BAD}-*dcpA* Δ*vps* showed significantly delayed detachment compared to the parent (Fig. 2*A*). As mentioned above, c-di-GMP is required to allosterically stimulate MshE activity (20). Previous studies have identified an MshE mutation that maintains activity even in the absence of c-di-GMP (MshE L10A/L54A/L58A, denoted MshE*) (20). If cell detachment is induced by a reduction in the activity of MshE (due to lowered c-di-GMP levels), we hypothesized that an

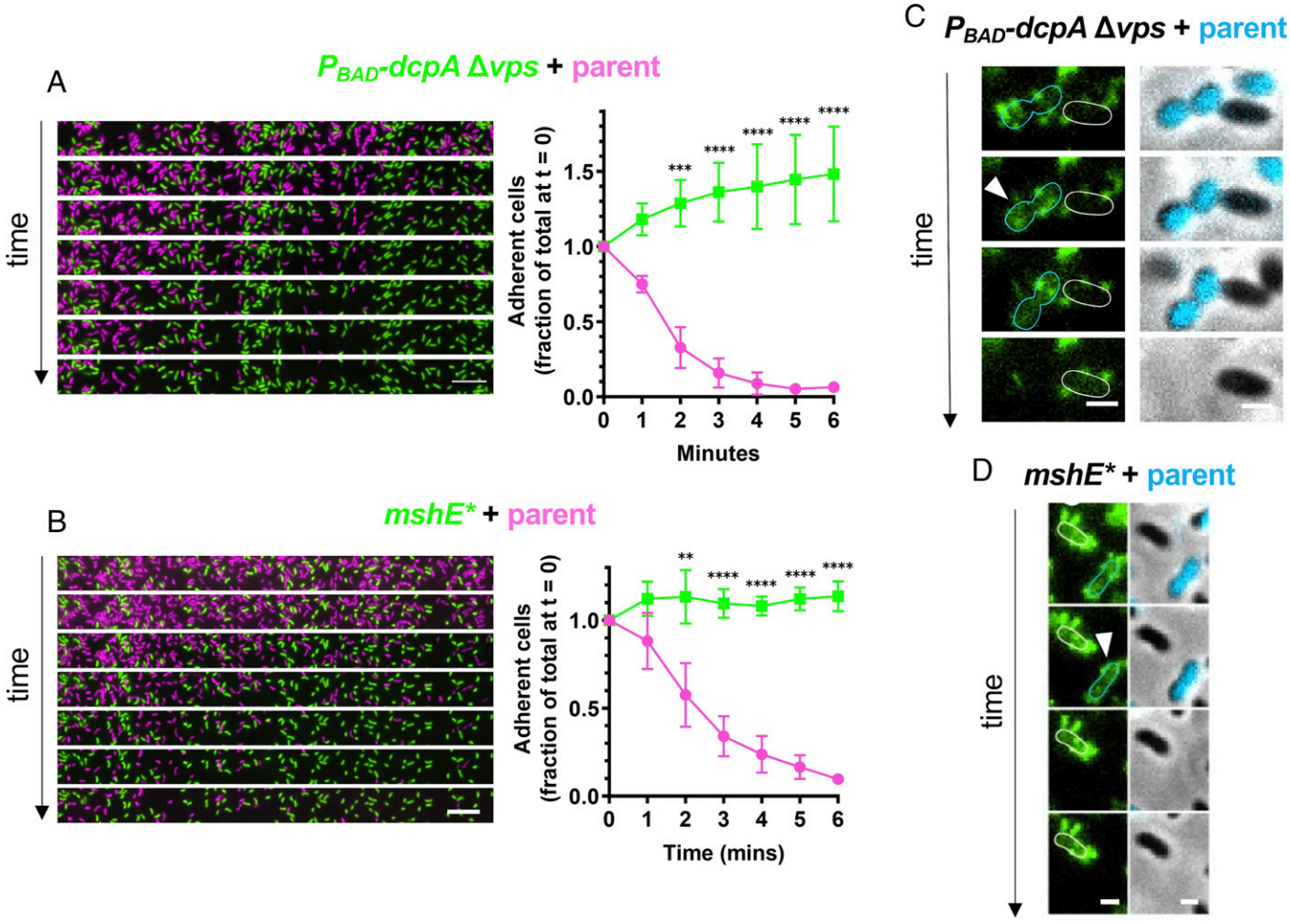

Fig. 2. Cell detachment is dependent on allosteric regulation of MshE activity by c-di-GMP. (*A*) MixD assay of P_{BAD}-*dcpA* Δ*vps* expressing GFP (green) and a parent strain expressing mCherry (fuchsia). P_{BAD}-*dcpA* Δ*vps* cells were induced with 0.15% arabinose. Representative montage shows time-lapse imaging (*Left*) with 1-min intervals between frames. Scale bar, 10 μm. The quantification of three biological replicates is shown in the line graph (*Right*) and is displayed as mean ± SD. Statistical comparisons were made by one-way ANOVA and post hoc Holm-Šídák test. $^{**}P < 0.01$, $^{***}P < 0.001$, $^{****}P < 0.0001$. Scale bar, 10 μm. (*B*) MixD assay as in *A* of *mshE** expressing GFP (green) and a parent strain expressing mCherry (fuchsia). (*C*) Representative montage shows time-lapse imaging of cells with AF488-mal-labeled MSHA pili. Cells represent a mixture of P_{BAD}-*dcpA* Δ*vps* cells and CyPet-expressing parent cells. P_{BAD}-*dcpA* Δ*vps* cells were induced with 0.15% arabinose as in *A*. Phase contrast images with overlaid CyPet fluorescence in cyan (*Right*) distinguish the mixed strains, and FITC fluorescence images in green (*Left*) show labeled pili. Parent cells are outlined in cyan, and P_{BAD}-*dcpA* Δ*vps* cells are outlined in white. White arrows indicate clear examples where pilus retraction precedes cell detachment. There are 20-s intervals between frames. Scale bar, 1 μm. (*D*) Representative montage shows time-lapse imaging of cells where pili are fluorescently labeled as in *C*. Cells represent a mixture of *mshE** cells and parent cells expressing cyan fluorescent protein (CFP). Parent cells are outlined in cyan and *mshE** cells are outlined in white.

MshE* mutation should delay or prevent cell detachment. Indeed, in a MixD assay, the MshE* strain showed a significant reduction in detachment compared to the parent (Fig. 2*B*). Consistent with MshE* bypassing c-di-GMP-dependent regulation, attachment of the MshE* strain is not altered even when an EAL-domain containing PDE, CdgJ, is overexpressed in this background (*SI Appendix*, Fig. S3). Also, direct labeling of pili in the P_{BAD}-*dcpA* Δ*vps* and MshE* strains demonstrated that cells maintained extended MSHA pili, which is consistent with a lack of pilus retraction in these backgrounds (Fig. 2 *C* and *D*). Together, these results suggest that cell detachment on slides is caused by MSHA pilus retraction in response to allosteric regulation of MshE by c-di-GMP.

Accumulation of a Volatile Signal Promotes Cell Detachment. Next, we sought to define the environmental stimulus that drives this detachment response. Because well slides were covered with an air-impermeable glass coverslip, we hypothesized that cells were responding to either the depletion or accumulation of a signal at the center of the well. Alternatively, it was possible that cells remained attached near the edge due to a physical property associated with that location on the well slide (e.g., the positive curvature or hydrophobic coating present at the edge of the well slide). To distinguish between these possibilities, we drilled holes into slides such that the centers of the wells were exposed to air. Under these conditions, cells detached as seen previously, except in the center of the well, where cells stayed bound around the hole (Fig. 3*A*). This suggests that attachment at the edge is not due to a physical property of the well slide and is instead a result of the depletion or accumulation of a signal in the center of the well.

As cells actively respire under these culture conditions, we hypothesized that they may rapidly deplete oxygen in the center of the well. To test this, we used oxygen-sensitive nanoparticles,

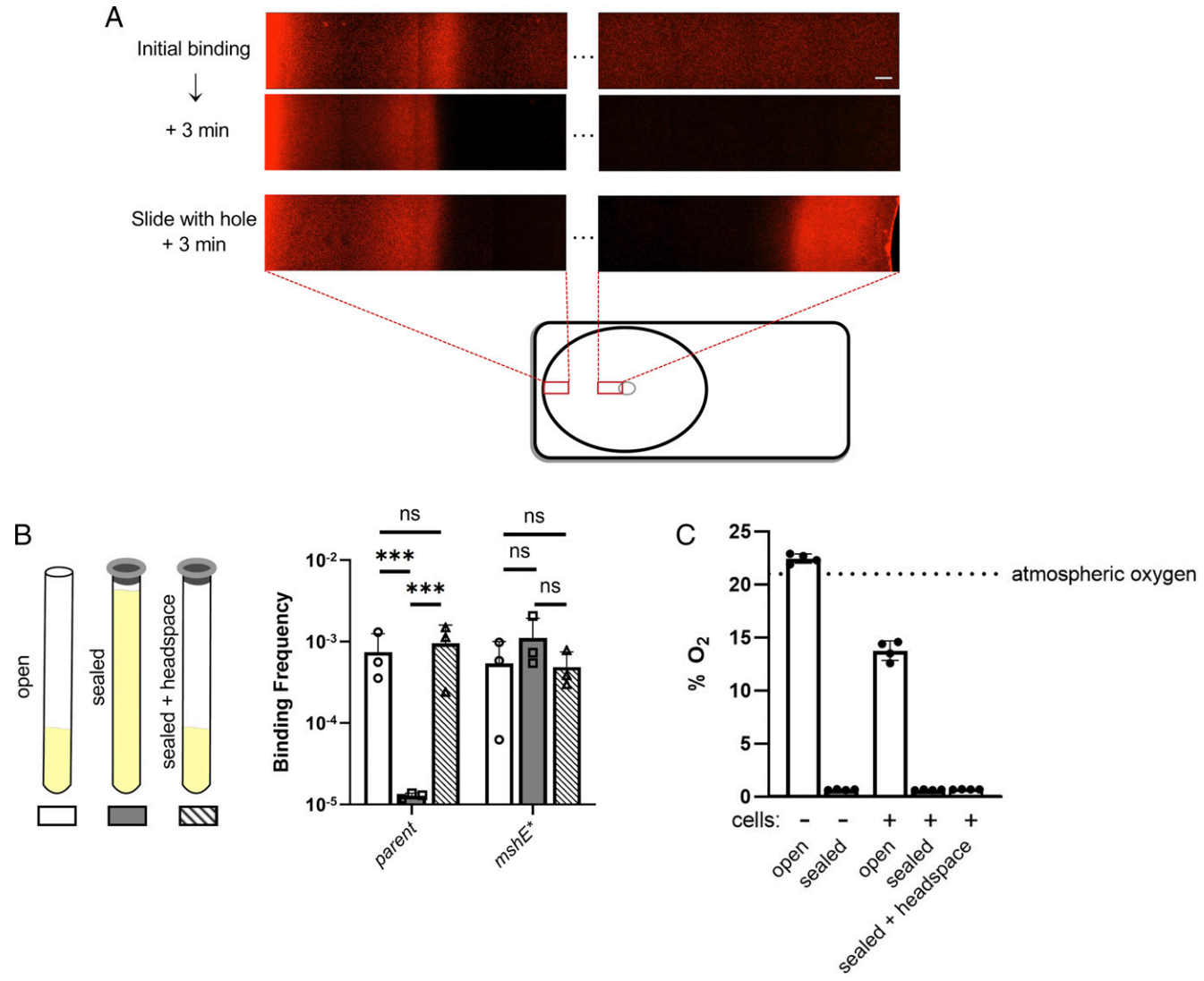

Fig. 3. Accumulation of a volatile signal promotes cell detachment. (*A*) Cell attachment was monitored in well slides by fluorescence microscopy with an mCherry-expressing parent strain. Wells either lacked (*Top* and *Middle*) or contained (*Bottom*) a hole in the center of the well, allowing for the open diffusion of volatiles. Five fields of view are omitted between the edge (*Left*) and center (*Right*) of the well. Scale bar, 50 μm. (*B*) Large-scale binding assays (*Right*) of cultures incubated in open tubes ("open"; white bars), an enclosed argon-flushed glass tube with low headspace ("sealed"; gray bars), or an enclosed argon-filled tube with abundant headspace ("sealed + headspace"; striped bars) (see diagram, *Left*). Data are from three independent biological replicates and shown as the mean ± SD. Statistical comparisons were made by one-way ANOVA and post hoc Holm-Šídák test. ***$P < 0.001$; ns, not significant. (*C*) Oxygen levels were measured under the same conditions used for *B*, using a noninvasive fiber optic oxygen meter. The initial % O_2 ("cells -") is indicated in the first two bars, and the % O_2 after incubation with cells ("cells +") is indicated in the remaining bars. Data are from four independent biological replicates and shown as the mean ± SD.

which exhibit strong phosphorescence specifically under low oxygen conditions (23–25). First, we confirmed that *V. cholerae* was able to deplete oxygen in the range detected by nanoparticles by using a plate reader (*SI Appendix*, Fig. S4*A*). We then added nanoparticles to a well slide and assessed the phosphorescence of nanoparticles at either the edge or center of the well. This revealed that live cells were indeed depleting oxygen in the center of the well (*SI Appendix*, Fig. S4*B*). While oxygen depletion in the center of the well correlates with cell detachment, these data do not demonstrate a causative relationship, and it remains possible that the accumulation of a volatile signal in the center of the well induces cell detachment.

To address the potential effects of oxygen in a controlled manner, we mimicked conditions that might be present at the edge of a well slide versus at the center by incubating cells in rolling glass rubes that were either open to the atmosphere ("open") or sealed under minimal argon headspace ("sealed"), respectively. We then measured the extent to which cells bound to the sides of the tubes under each condition. We confirmed that these culture conditions recapitulated the binding phenotypes seen in the MixD assays, where the parent strain bound well in open conditions (which mimics the edge of the well) and poorly under sealed conditions (which mimics the center of a well slide) (Fig. 3*B*). Conversely, the MshE* mutant bound equally well under both open and sealed conditions (Fig. 3*B*). The poor binding of the parent in the sealed tubes could be due to either (1) an absence of oxygen, if oxygen depletion is the inducing cue for cell detachment, or (2) the accumulation of a volatile compound that induces cell detachment. To distinguish between these possibilities, we assessed the attachment of cells in a sealed, rolling, argon-flushed tube with increased headspace ("sealed + headspace"). We reasoned that if oxygen depletion is the inducing signal, then the parent strain should still bind poorly under these conditions, since they will still be oxygen depleted. However, if a volatile compound induces cell detachment, then the inclusion of ample headspace should allow for the diffusion of that signal away from the culture, preventing it from accumulating to the levels required to induce cell detachment. When we performed this experiment, we found that the attachment of the parent phenocopied the open culture tube (Fig. 3*B*). Importantly, we demonstrate that cells incubated under these culture conditions were, indeed, depleted of oxygen (Fig. 3*C*). Together, this indicates that oxygen depletion is not sufficient to induce cell detachment and further suggests that the accumulation of a volatile signal is likely responsible for inducing cell detachment. Importantly, the MshE* mutant bound similarly under all conditions, indicating that the different experimental conditions tested only impacted cell attachment through modulation of MSHA pilus dynamic activity.

Cell Detachment Requires the PDE CdpA. Thus far, our data suggest that the accumulation of a volatile signal induces MSHA pilus retraction in a manner that depends on a decrease in cellular c-di-GMP. We, therefore, hypothesized that *V. cholerae* carries a PDE that, under sealed conditions, decreases c-di-GMP levels, triggering MSHA pilus retraction and cell detachment. We would expect a mutant lacking this putative PDE to exhibit enhanced adherence under large-scale sealed conditions (akin to the MshE* mutant). To test this hypothesis, we carried out a genetic selection to isolate transposon mutants that exhibited enhanced adherence under sealed conditions. Following the genetic selection, we isolated 10 colonies and sequenced the transposon-genomic junction in each. All mutants contained transposon insertions (9 distinct mutations) in *cdpA* (VC0130) (*SI Appendix*, Fig. S5*A*). CdpA is a functional PDE that contains a NosP sensory domain (26, 27). Deleting *cdpA* in a clean background recapitulated the improved binding under sealed conditions that was originally selected for (*SI Appendix*, Fig. S5*B*), and in a MixD assay, the Δ*cdpA* mutant exhibited significantly delayed detachment compared to the parent strain (Fig. 4*A*). Importantly, this phenotype could be complemented *in trans* with a single copy of *cdpA* integrated at an ectopic location under the control of its native promoter (Δ*cdpA* Δ*lacZ*::*cdpA*^{WT}) (Fig. 4*B*). These results confirm that CdpA plays an important role in cell detachment under sealed conditions.

Because CdpA is a PDE, we hypothesized that it reduced c-di-GMP under sealed conditions to promote MSHA pilus retraction and subsequent cell detachment. To test this, we first mutated the EAL domain in *cdpA* (*cdpA* has ECL instead of the canonical EAL sequence). In MixD assays, the Δ*cdpA* Δ*lacZ*::*cdpA*$^{ECL\rightarrow AAA}$ strain phenocopied the Δ*cdpA* mutant (Fig. 4*C*), indicating that the PDE activity of CdpA plays a critical role in promoting cell detachment. Consistent with this result, we found that intracellular levels of c-di-GMP measured by liquid chromatography-tandem mass spectrometry (LC-MS/MS) were reduced under sealed conditions in a CdpA-dependent manner (Fig. 4*D*).

Based on the data described above, CdpA likely degrades c-di-GMP specifically under sealed conditions. What remains unclear is the mechanism by which CdpA activity is stimulated. One possibility is that upon accumulation of the volatile signal, CdpA protein levels are increased. To test this hypothesis, we generated a functional *cdpA*-3xFLAG strain (*SI Appendix*, Fig. S5*C*) and assessed protein levels by Western blot. This revealed that total CdpA protein levels did not differ when cells were incubated in open vs. sealed conditions (Fig. 4*E*). This suggests that CdpA-dependent detachment is not due to the regulation of CdpA expression but is instead likely due to posttranslational regulation of CdpA activity.

Nitric Oxide (NO) Is Necessary and Sufficient to Promote MSHA Pilus Retraction and Cell Detachment in a CdpA-Dependent Manner. CdpA encodes a NosP domain, which has recently been shown to bind heme in a manner that alters its PDE activity (27). NosP domains have previously been implicated in sensing NO (28), and bacterial NO production generally occurs under microaerobic conditions (29, 30). Thus, we hypothesized that MSHA retraction and CdpA activity may be occurring due to NO production under sealed, microaerobic conditions. Therefore, we tested whether NO was necessary and sufficient to induce CdpA-dependent detachment. To determine if NO was necessary for detachment, we incubated cells on slides with the NO scavenger 2-phenyl-4,4,5,5,-tetramethylimidazoline-1-oxyl 3-oxide (PTIO). In the presence of PTIO, parent cells remained attached to the surface in a manner that resembled the Δ*cdpA* mutant (Fig. 5*A*). To exclude the possibility that PTIO was nonspecifically scavenging reactive oxygen species (ROS) (31), we also assessed the impact of the ROS-specific scavenger Tiron. Tiron did not inhibit the detachment of the parent strain, suggesting that PTIO inhibits cell detachment by specifically scavenging NO or a related molecule (Fig. 5*A*). To test if NO was sufficient to induce detachment, we incubated cells with the NO donor diethylamine-NONOate (DEA-NONOate) and assessed cell attachment under aerobic conditions. We found that parent cells attached poorly in the presence of DEA-NONOate, whereas attachment of the Δ*cdpA* mutant was unaffected (Fig. 5*B*). Furthermore, incubation with DEA-NONOate resulted in MSHA pilus retraction in a CdpA-dependent manner (Fig. 5*C*). This condition, however, did not alter CdpA expression, further indicating that CdpA activity is likely regulated posttranslationally (*SI Appendix*, Fig. S6*A*). Together, these observations are consistent with NO being necessary and sufficient to induce MSHA pilus retraction through activation of CdpA.

Next, we wanted to determine how widespread this CdpA-dependent activity may be. A phylogenetic analysis revealed that

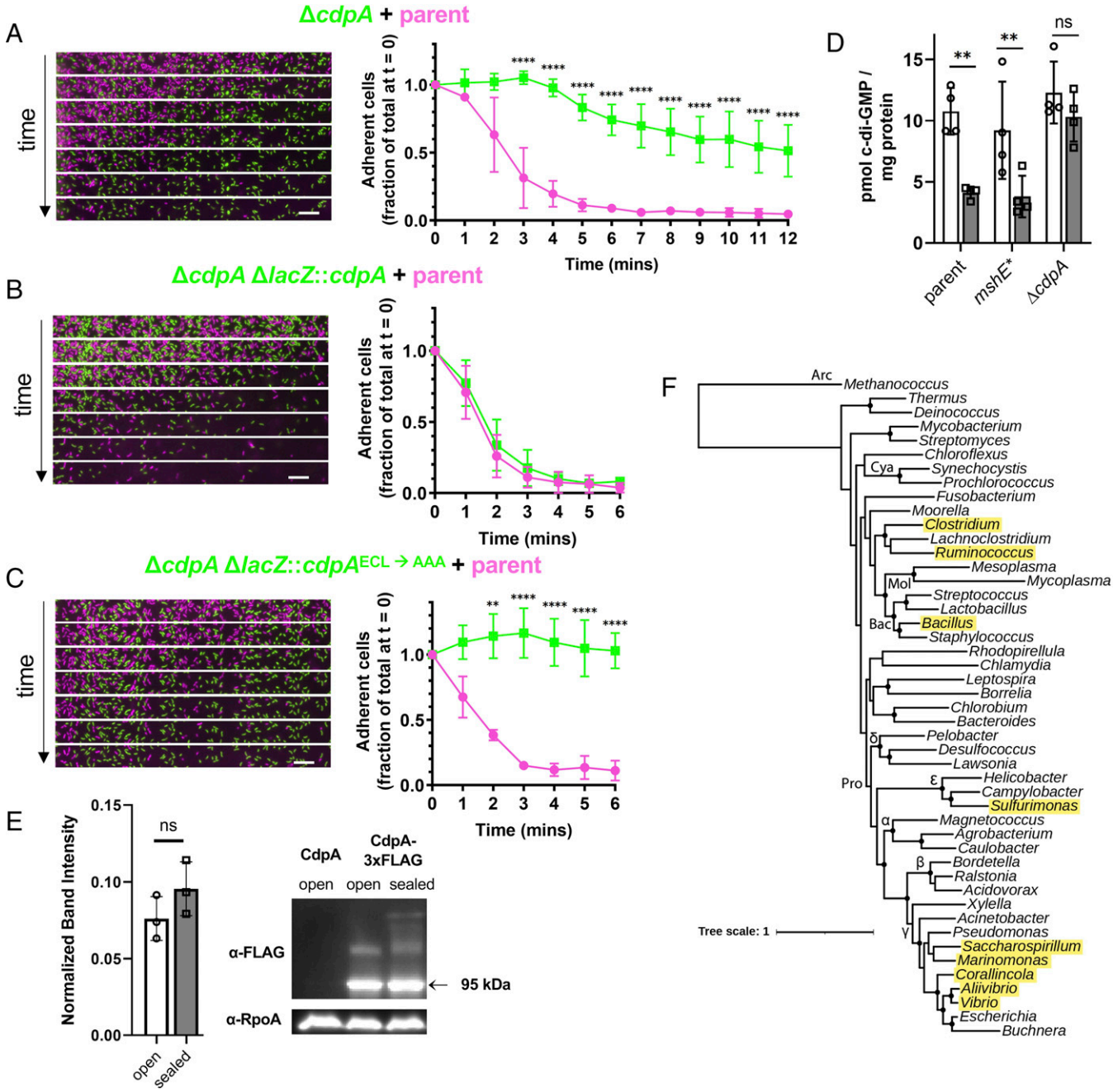

Fig. 4. CdpA is a PDE that promotes cell detachment under sealed conditions. (*A*–*C*) Show MixD assays of the indicated strains. Cells expressed GFP (green) or mCherry (fuchsia) as indicated by the color-coded genotypes. Complemented strains are denoted by Δ*lacZ::cdpA*, indicating that a copy of *cdpA* along with its native promoter were introduced at an ectopic site on the chromosome. Representative montages of time-lapse imaging (*Left*) display 1-min intervals between frames. Scale bar, 10 μm. Quantification of three biological replicates is shown in each line graph (*Right*). (*D*) Quantification of intracellular c-di-GMP concentrations in the indicated strains. Data are from four independent biological replicates. White bars represent samples from open tubes, while gray bars indicate samples from sealed tubes. (*E*) Representative Western blot (*Right*) and quantification (*Left*) were used to assess CdpA protein levels under open and sealed conditions. Band intensities are normalized to the RpoA loading control. Data are from three independent experiments. (*F*) Conservation of CdpA across bacterial species. The estimated maximum likelihood phylogeny of the indicated microbes is based on a concatenated alignment of 36 conserved proteins identified from whole-genome sequences. Genera with members that contain a CdpA homolog are highlighted in yellow. Major taxa are labeled along their nodes. Pro, Proteobacteria (Greek letters indicate subdivisions); Bac, Bacilli; Mol, Mollicutes; Cya, Cyanobacteria; Arc, Archaea. Scale bar indicates distance. All graphs display mean ± SD. Statistical comparisons were made by one-way ANOVA and post hoc Holm-Šídák test. $^{**}P < 0.01$, $^{****}P < 0.0001$; ns, not significant.

CdpA is largely conserved among the *Vibrionaceae* and is also prevalent in *Aliivibrio* species (*SI Appendix*, Figs. S7 and S8). Based on sequence similarity and presence within the *Vibrio* and *Aliivibrio*, we conclude that these are homologs with a conserved functional role. Furthermore, we found *cdpA* homologs in phylogenetically distant species (e.g., *Clostridium* and *Bacillus*) (Fig. 4*F*; *SI Appendix*, Fig. S9 and Dataset S1). Thus, it is tempting to speculate that CdpA may be a widely conserved NO-responsive PDE.

Above, our data suggest that CdpA may be posttranslationally regulated. Because the heme-bound NosP domain of CdpA

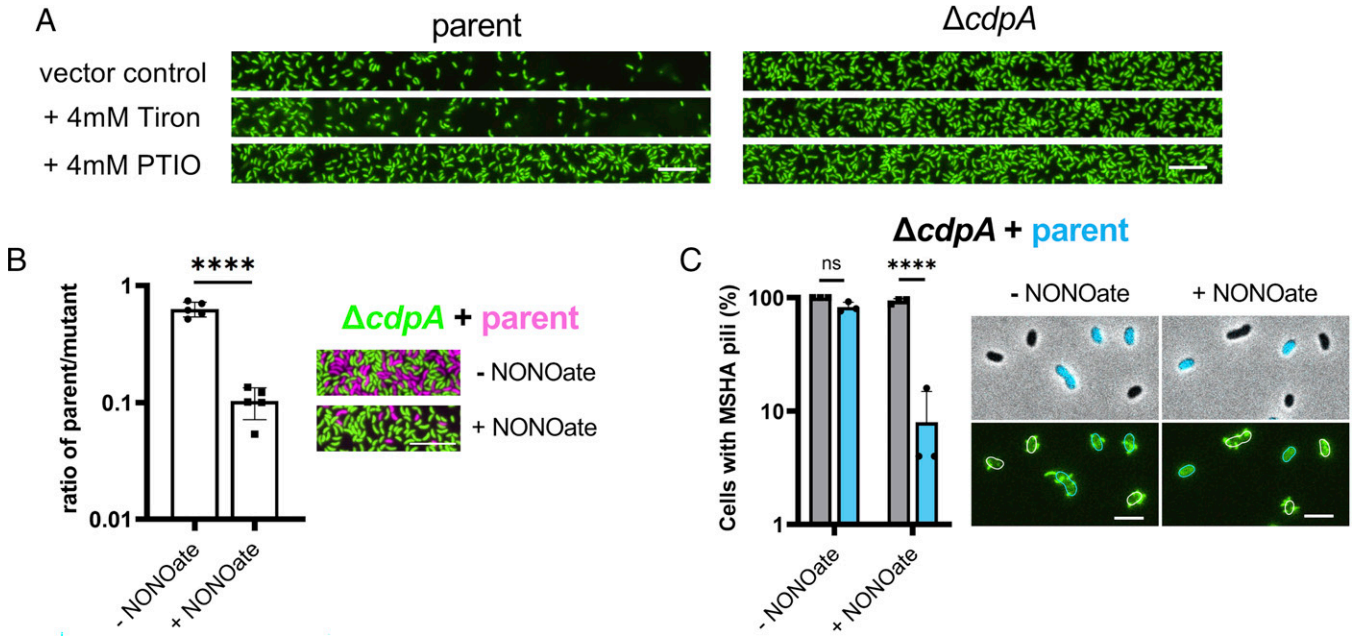

Fig. 5. Nitric oxide stimulates detachment in a CdpA-dependent manner. (*A*) Representative images of detachment of GFP-expressing parent or Δ*cdpA* strains after incubation with Tiron (4 mM), PTIO (4 mM), or dimethyl sulfoxide (DMSO) as a vector control. Scale bar, 10 μm. (*B*) Quantification (*Left*) of initial attachment for a 1:1 mixture of the mCherry-expressing parent strain (fuchsia) and GFP-expressing Δ*cdpA* mutant strain (green) when incubated in the presence or absence of 200 μM DEA-NONOate, as indicated. The ratio was determined by dividing the number of attached parent cells (fuchsia) by the number of attached mutant cells (green) as depicted in the representative image on the right. Data are from 5 independent experiments with at least 270 cells analyzed per replicate and are shown as the mean ± SD. The statistical comparison was made by Student's *t* test. Scale bar, 10 μm. (*C*) Quantification (*Left*) of parent (blue) or Δ*cdpA* (gray) piliation after incubation in the presence or absence of 200 μM DEA-NONOate. Data are presented as the percent of cells that exhibited surface piliation. Data are from 3 independent experiments with at least 50 cells analyzed per replicate and are shown as the mean ± SD. Representative images (*Right*) of cells with AF488-mal-labeled MSHA pili. Cells represent a mixture of Δ*cdpA* cells and CyPet-expressing parent cells. Phase contrast images with overlaid CyPet fluorescence in cyan (*Top*) distinguish the mixed strains, and FITC fluorescence images in green (*Bottom*) show labeled pili. Parent cells are outlined in cyan and Δ*cdpA* cells are outlined in white. Scale bar, 3 μm. The statistical comparison was made by one-way ANOVA and post hoc Holm-Šídák test. ****$P < 0.0001$; ns, not significant.

is implicated in reacting with NO, we also assessed the impact of NO on the PDE activity of purified heme-bound CdpA. The status of the heme-bound CdpA was confirmed through ultraviolet/visible (UV/Vis) spectroscopy and an analysis of Soret bands (*SI Appendix*, Fig. S6*B*). Specifically, the Soret band around 420 nm confirmed the presence of CdpA bound to ferrous (Fe^{II}) heme, and a broader Soret band, shifted to around 395 nm, indicated the presence of the Fe^{II}-NO complex as previously described (27). In vitro PDE assays of these samples, however, showed that there was only a slight and inconsistent increase in PDE activity for Fe^{II}-NO CdpA compared to Fe^{II}-CdpA (*SI Appendix*, Fig. S6*C*). This discrepancy between the lack of NO-stimulated CdpA activity in vitro and the strong NO-stimulated CdpA activity in vivo may be due to limitations of the in vitro setup. While the heme moiety used for this experiment (heme b) matches what was observed natively bound to other NosP-containing proteins purified from *Escherichia coli* (28), CdpA may bind a different heme moiety in vivo. Alternatively, there may be an unidentified cofactor required for CdpA activity which is present in vivo but lacking in our in vitro assays. In support of this hypothesis, we show that CdpA PDE activity is very poor in vitro (requires overnight incubations) (*SI Appendix*, Fig. S6*C*), despite the fact that it exerts its effect in vivo within just a few minutes (Fig. 4).

A major tenet of our model is that *V. cholerae* endogenously generates NO under sealed conditions to stimulate CdpA activity. An important caveat preventing this conclusion, however, is that *V. cholerae* lacks the canonical denitrification pathway that allows many bacterial species to generate NO. Furthermore, it lacks the dissimilatory nitrate reduction to ammonium (DNRA) pathway, which can produce NO as a minor byproduct. Although *V. cholerae* does encode a nitrate reductase (in the *nap* operon) that converts nitrate to nitrite, it lacks homologs of other denitrification or DNRA enzymes (32, 33). While *V. cholerae* encounters NO during infection (34–36), it is not thought to generate NO endogenously. A MixD analysis of a Δ*nap* mutant (37) (*SI Appendix*, Fig. S10*A*) was indistinguishable from the parent (*SI Appendix*, Fig. S10*B*), suggesting that nitrate reductase activity is not required to generate a molecular cue for cell detachment. Thus, if NO is being generated, it must be through a pathway previously uncharacterized in *V. cholerae*.

To test whether *V. cholerae* was actually generating NO, we incubated cells with diaminorhodamine-4M acetoxymethyl ester (DAR-4M AM), an NO-specific fluorescent probe. Using DAR-4M AM, we readily measured NO produced by DEA-NONOate (*SI Appendix*, Fig. S10*C*) and *E. coli*, which has an intact DNRA pathway, but were unable to detect NO production from *V. cholerae*, even when cells were incubated under the sealed conditions that induce cell detachment (*SI Appendix*, Fig. S10*D*). Importantly, NO was still detected by DAR-4M AM when *E. coli* cells (grown under conditions where they do not generate NO) were mixed with DEA-NONOate, albeit to a reduced level. These data suggest that cells may slightly decrease the threshold for NO detection by DAR-4M AM by acting as an NO sponge. Thus, it remains feasible that concentrations of NO lower than our limit of detection in the presence of cells (i.e., 40 μM DEA-NONOate) are generated in *V. cholerae*. Furthermore, there is evidence that extracellular NO may not equilibrate with cytoplasmic levels (38), allowing for the possibility that NO generated endogenously by *V. cholerae* may be at levels too low to be measured by this technique. Alternatively, *V. cholerae* may be generating a distinct, NO-like

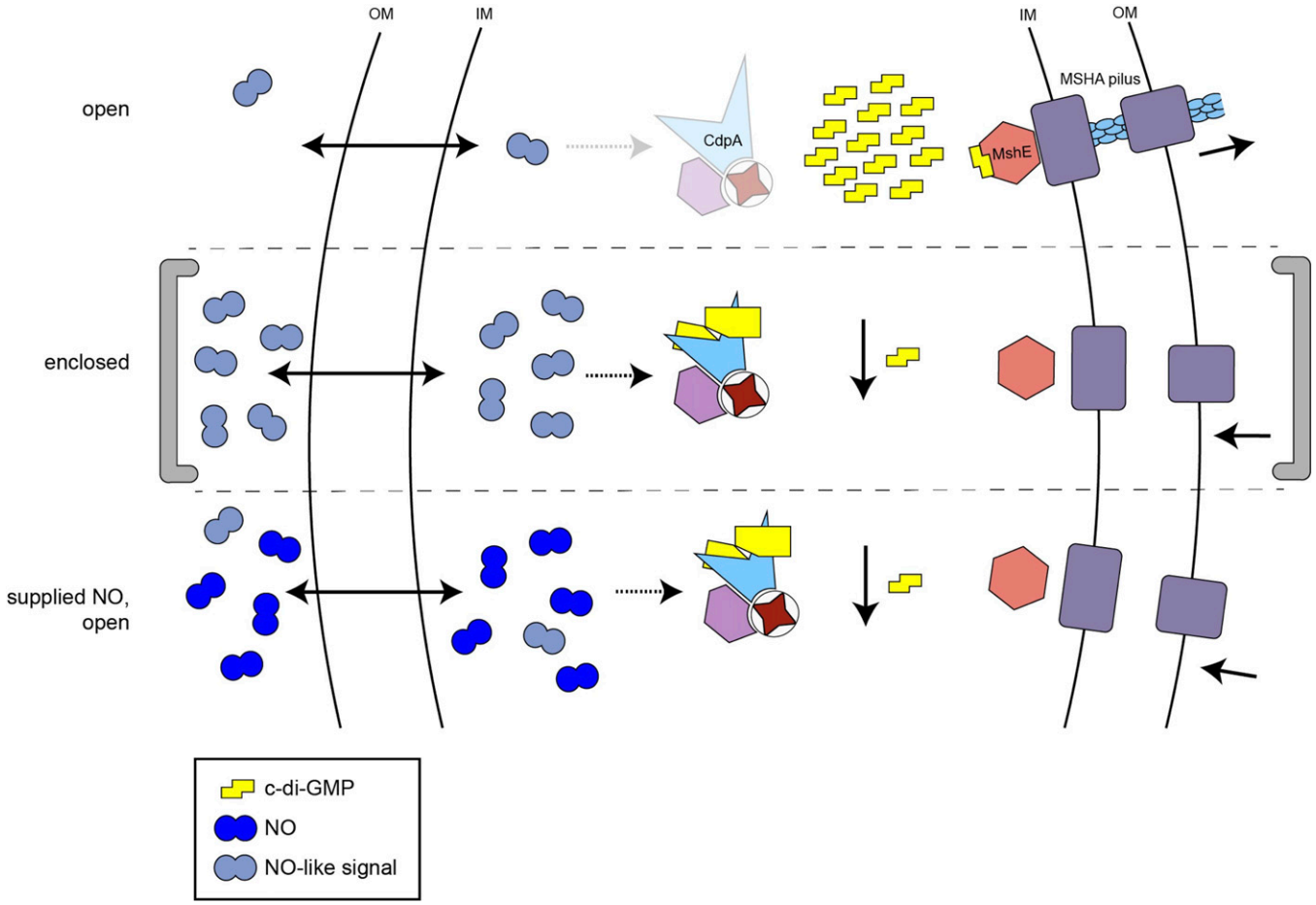

Fig. 6. Proposed model for CdpA-dependent induction of MSHA pilus retraction. Under open conditions (*Top*), volatiles (including the NO-like signal molecule) diffuse across the cell membrane and away from cells. CdpA remains inactive, and intracellular c-di-GMP levels stay elevated. This stimulates MshE activity, which causes the extension of MSHA pili and attachment of cells to a surface. Under sealed conditions (*Middle*), the NO-like signal accumulates. This signal, along with a potential cofactor (depicted in lavender), stimulate the PDE activity of CdpA. This decreases the intracellular concentration of c-di-GMP, prompting the retraction of MSHA pili and detachment of cells from the surface. Exogenously added NO (*Bottom*) can also diffuse into the cell and stimulate CdpA activity, resulting in decreased c-di-GMP, retraction of MSHA pili, and cell detachment. IM, inner membrane; OM, outer membrane.

molecule that promotes cell detachment under sealed conditions. This could explain why NO was not able to strongly stimulate CdpA PDE activity in vitro (*SI Appendix*, Fig. S6*C*) and why NO was not detected by DAR-4M AM in cells incubated under sealed conditions (*SI Appendix*, Fig. S10*D*). Defining the precise environmental signals and cofactors required to stimulate CdpA PDE activity will be a focus of future work. While our data indicate that NO is sufficient to stimulate cell detachment in *V. cholerae* (Fig. 5*B*), the means by which NO (or an NO-like molecule) is endogenously generated remains unclear.

Discussion

While the frequency and timing of pilus extension and retraction are crucial to their function, many questions remain about how pilus dynamics are regulated. Some progress has been made on this front, including the characterization of regulators that impact dynamic activity (39–42) and the impact of spatial organization of the extension and retraction motors (43–45). Our study highlights another mode of regulation for pilus dynamic activity, wherein environmental regulatory cues rapidly induce pilus retraction through the modulation of a secondary messenger (c-di-GMP) that is required for pilus biogenesis. Specifically, our findings describe a pathway by which NO (or an NO-like signal) stimulates the PDE activity of CdpA to reduce cellular concentrations of c-di-GMP, which ultimately induces the retraction of MSHA pili and detachment of *V. cholerae* from a surface (Fig. 6).

CdpA is only one of at least 62 enzymes that contribute to c-di-GMP production and/or degradation in *V. cholerae* (46). These diverse DGCs and PDEs are believed to respond to distinct signals/cues, thus allowing cells to modulate c-di-GMP under different environmental conditions (18). While inducing signals have been determined for some of these enzymes (47–49), the complex regulatory interplay between them is largely uncharacterized, and many of the environmental cues required to stimulate their activities remain unclear. Here, we uncover that CdpA responds to externally supplied NO and an endogenously generated NO-like signal to reduce intracellular c-di-GMP. Production of this signal takes place under sealed conditions where a volatile signal can accumulate. It is unclear whether oxygen depletion is a prerequisite for the production of the signal, but the accumulation of the signal in an enclosed environment (under which cells also deplete oxygen) is required for CdpA activation and c-di-GMP depletion. One outcome for this response is the retraction of MSHA pili, which results in cell detachment.

The specific identity of the endogenously generated signal is still unknown, as well as the genetic factors that are needed to

generate this signal. This is due, in part, to limitations of our genetic selection. Although our mutant population may have contained strains that were unable to generate the NO-like signal, performing the selection on pooled mutants meant that many other cells (with mutations in other genes) were still able to make the signal. Thus, mutant cells deficient for generating the signal were still exposed to the signal generated by their neighbors *in trans*, which could induce their detachment and prevent them from being identified in our selection. It is also possible that the pathway that generates this NO-like signal is essential for viability, which could complicate uncovering the genes responsible through classical genetic approaches.

MSHA pili are principally required by *V. cholerae* to form biofilms in the aquatic environment. Retraction of MSHA pili in the presence of NO, however, may also be biologically relevant when this facultative pathogen infects its human host. The expression of MSHA pili during infection is known to attenuate *V. cholerae* due to the propensity of these appendages to bind secretory IgA in the gut, which promotes their clearance from the small intestine (50). As a result, MSHA pili are highly regulated during infection. Expression of the MSHA locus is downregulated (50, 51), turning off the future production of MSHA pili. Additionally, MshA pilin pools in the inner membrane are degraded upon the production of toxin coregulated pili, which are specifically expressed during infection (51). NO-induced MSHA pilus retraction could provide a third layer of regulation, ensuring the rapid elimination of any surface-accessible MSHA pili. As the small intestine is a high-NO environment (52, 53), we speculate that this cue could represent an important trigger to induce rapid MSHA pilus retraction, contributing to the ability of *V. cholerae* to evade the host innate immune response during infection.

Materials and Methods

A detailed description of materials and methods can be found in the *SI Appendix, Materials and Methods*, including the following: bacterial strains and culture conditions, construction of mutant strains, transposon mutagenesis and selection, microscopy and image analysis, MixD analysis, assessment of cell attachment, visualization of labeled pili, oxygen quantification, c-di-GMP quantification, Western blotting, phylogenetic analysis, detection of NO in liquid culture, CdpA purification and in vitro PDE activity assays, Δ*nap* growth assay, and statistics.

Data Availability. All study data are included in the article and/or supporting information.

ACKNOWLEDGMENTS. We thank Clay Fuqua, Julia van Kessel, Tuli Mukhophadyay, Ilana Heckler, Sidney L Shaw, and Emily Weinert for helpful discussions, as well as Istvan Katona for generous access to their microscope. This work was supported in part by Grants R35GM128674 (to A.B.D.), R01AI102584 (to F.H.Y.), GM118894 (to E.M.B.), R01GM113121 (to S.C.J.), and R01CA167250 (C.L.F.) from the NIH. J.B.M. is supported by a National Science Foundation CAREER award, Grant MCB-1749489. Y.V.B. is supported by the Canada 150 Research Chair from the Canadian Institutes of Health Research.

1. R. Denise, S. S. Abby, E. P. C. Rocha, Diversification of the type IV filament superfamily into machines for adhesion, protein secretion, DNA uptake, and motility. *PLoS Biol.* **17**, e3000390. (2019).
2. C. K. Ellison *et al.*, Retraction of DNA-bound type IV competence pili initiates DNA uptake during natural transformation in *Vibrio cholerae*. *Nat. Microbiol.* **3**, 773–780 (2018).
3. A. J. Merz, M. So, M. P. Sheetz, Pilus retraction powers bacterial twitching motility. *Nature* **407**, 98–102 (2000).
4. G. A. O'Toole, R. Kolter, Flagellar and twitching motility are necessary for *Pseudomonas aeruginosa* biofilm development. *Mol. Microbiol.* **30**, 295–304 (1998).
5. C. K. Ellison *et al.*, Obstruction of pilus retraction stimulates bacterial surface sensing. *Science* **358**, 535–538 (2017).
6. C. Berne, C. K. Ellison, A. Ducret, Y. V. Brun, Bacterial adhesion at the single-cell level. *Nat. Rev. Microbiol.* **16**, 616–627 (2018).
7. L. Craig, M. E. Pique, J. A. Tainer, Type IV pilus structure and bacterial pathogenicity. *Nat. Rev. Microbiol.* **2**, 363–378 (2004).
8. L. Craig, K. T. Forest, B. Maier, Type IV pili: Dynamics, biophysics and functional consequences. *Nat. Rev. Microbiol.* **17**, 429–440 (2019).
9. M. McCallum, S. Tammam, A. Khan, L. L. Burrows, P. L. Howell, The molecular mechanism of the type IVa pilus motors. *Nat. Commun.* **8**, 15091 (2017).
10. Y. W. Chang *et al.*, Architecture of the type IVa pilus machine. *Science* **351**, aad2001 (2016).
11. P. I. Watnick, K. J. Fullner, R. Kolter, A role for the mannose-sensitive hemagglutinin in biofilm formation by *Vibrio cholerae* El Tor. *J. Bacteriol.* **181**, 3606–3609 (1999).
12. P. I. Watnick, R. Kolter, Steps in the development of a *Vibrio cholerae* El Tor biofilm. *Mol. Microbiol.* **34**, 586–595 (1999).
13. K. L. Meibom *et al.*, The Vibrio cholerae chitin utilization program. *Proc. Natl. Acad. Sci. U.S.A.* **24**, 2524–2529 (2004).
14. K. A. Floyd *et al.*, c-di-GMP modulates type IV MSHA pilus retraction and surface attachment in Vibrio cholerae. *Nat. Commun.* **11**, 1549 (2020).
15. C. B. Whitchurch, M. Hobbs, S. P. Livingston, V. Krishnapillai, J. S. Mattick, Characterisation of a *Pseudomonas aeruginosa* twitching motility gene and evidence for a specialised protein export system widespread in eubacteria. *Gene* **101**, 33–44 (1991).
16. J. L. Chlebek *et al.*, PilT and PilU are homohexameric ATPases that coordinate to retract type IVa pili. *PLoS Genet.* **15**, e1008448 (2019).
17. D. W. Adams, J. M. Pereira, C. Stoudmann, S. Stutzmann, M. Blokesch, The type IV pilus protein PilU functions as a PilT-dependent retraction ATPase. *PLoS Genet.* **15**, e1008393 (2019).
18. U. Jenal, J. Malone, Mechanisms of cyclic-di-GMP signaling in bacteria. *Annu. Rev. Genet.* **40**, 385–407 (2006).
19. C. J. Jones *et al.*, C-di-GMP regulates motile to sessile transition by modulating MshA pili biogenesis and near-surface motility behavior in *Vibrio cholerae*. *PLoS Pathog.* **11**, e1005068 (2015).
20. Y.-C. Wang *et al.*, Nucleotide binding by the widespread high-affinity cyclic di-GMP receptor MshEN domain. *Nat. Commun.* **7**, 12481 (2016).
21. A. Nakhamchik, C. Wilde, D. A. Rowe-Magnus, Cyclic-di-GMP regulates extracellular polysaccharide production, biofilm formation, and rugose colony development by *Vibrio vulnificus*. *Appl. Environ. Microbiol.* **74**, 4199–4209 (2008).
22. J. C. Fong, F. H. Yildiz, The rbmBCDEF gene cluster modulates development of rugose colony morphology and biofilm formation in *Vibrio cholerae*. *J. Bacteriol.* **189**, 2319–2330 (2007).
23. H. A. Arjes *et al.*, Biosurfactant-mediated membrane depolarization maintains viability during oxygen depletion in *Bacillus subtilis*. *Curr. Biol.* **30**, 1011–1022.e6. (2020).
24. C. A. DeRosa *et al.*, Oxygen sensing difluoroboron dinaphthoylmethane polylactide. *Macromolecules* **48**, 2967–2977 (2015).
25. C. A. DeRosa *et al.*, Oxygen sensing difluoroboron β-diketonate polylactide materials with tunable dynamic ranges for wound imaging. *ACS Sens.* **1**, 1366–1373 (2016).
26. R. Tamayo, S. Schild, J. T. Pratt, A. Camilli, Role of cyclic Di-GMP during el tor biotype Vibrio cholerae infection: Characterization of the in vivo-induced cyclic Di-GMP phosphodiesterase CdpA. *Infect. Immun.* **76**, 1617–1627 (2008).
27. I. Heckler, S. Hossain, E. M. Boon, Heme inhibits the activity of a c-di-GMP phosphodiesterase in *Vibrio cholerae*. *Biochem. Biophys. Res. Commun.* **529**, 1112–1116 (2020).
28. S. Hossain, E. M. Boon, Discovery of a novel nitric oxide binding protein and nitric-oxide-responsive signaling pathway in *Pseudomonas aeruginosa*. *ACS Infect. Dis.* **3**, 454–461 (2017).
29. W. G. Zumft, Cell biology and molecular basis of denitrification. *Microbiol. Mol. Biol. Rev.* **61**, 533–616 (1997).
30. S. Rinaldo, G. Giardina, F. Mantoni, A. Paone, F. Cutruzzolà, Beyond nitrogen metabolism: Nitric oxide, cyclic-di-GMP and bacterial biofilms. *FEMS Microbiol. Lett.* **365**, fny029 (2018).
31. S. Goldstein, A. Russo, A. Samuni, Reactions of PTIO and carboxy-PTIO with *NO, *NO2, and O2-*. *J. Biol. Chem.* **278**, 50949–50955 (2003).
32. E. Bueno, V. Pinedo, F. Cava, Adaptation of *Vibrio cholerae* to hypoxic environments. *Front. Microbiol.* **11**, 739 (2020).
33. E. Bueno, B. Sit, M. K. Waldor, F. Cava, Genetic dissection of the fermentative and respiratory contributions supporting *Vibrio cholerae* hypoxic growth. *J. Bacteriol.* **202**, e00243-20 (2020).
34. E. N. Janoff *et al.*, Nitric oxide production during *Vibrio cholerae* infection. *Am. J. Physiol. Gastrointest. Liver Physiol.* **273**, G1160-7 (1997).
35. B. W. Davies *et al.*, DNA damage and reactive nitrogen species are barriers to *Vibrio cholerae* colonization of the infant mouse intestine. *PLoS Pathog.* **7**, e1001295 (2011).
36. A. M. Stern *et al.*, The NorR regulon is critical for *Vibrio cholerae* resistance to nitric oxide and sustained colonization of the intestines. *MBio* **3**, e00013-12 (2012).
37. E. Bueno, B. Sit, M. K. Waldor, F. Cava, Anaerobic nitrate reduction divergently governs population expansion of the enteropathogen *Vibrio cholerae*. *Nat. Microbiol.* **3**, 1346–1353 (2018).
38. C. E. Vine, S. K. Purewal, J. A. Cole, NsrR-dependent method for detecting nitric oxide accumulation in the *Escherichia coli* cytoplasm and enzymes involved in NO production. *FEMS Microbiol. Lett.* **325**, 108–114 (2011).
39. M. Shah *et al.*, A phage-encoded anti-activator inhibits quorum sensing in *Pseudomonas aeruginosa*. *Mol. Cell* **81**, 571–583.e6 (2021).

40. R. Mercier *et al.*, The polar Ras-like GTPase MglA activates type IV pilus via SgmX to enable twitching motility in *Myxococcus xanthus*. *Proc. Natl. Acad. Sci. U.S.A.* **117**, 28366–28373 (2020).
41. R. J. Scheffler *et al.*, Pseudomonas aeruginosa detachment from surfaces via a self-made small molecule. *J. Biol. Chem.* **296**, 100279 (2021).
42. C. K. Ellison *et al.*, *Acinetobacter baylyi* regulates type IV pilus synthesis by employing two extension motors and a motor protein inhibitor. *Nat. Commun.* **12**, 3744 (2021).
43. P. A. DeLange, T. L. Collins, G. E. Pierce, J. B. Robinson, PilJ localizes to cell poles and is required for type IV pilus extension in *Pseudomonas aeruginosa*. *Curr. Microbiol.* **55**, 389–395 (2007).
44. I. Bulyha *et al.*, Regulation of the type IV pili molecular machine by dynamic localization of two motor proteins. *Mol. Microbiol.* **74**, 691–706 (2009).
45. M. J. Kühn *et al.*, Mechanotaxis directs *Pseudomonas aeruginosa* twitching motility. *Proc. Natl. Acad. Sci. U.S.A.***118**, e2101759118 (2021).
46. J. G. Conner, D. Zamorano-Sánchez, J. H. Park, H. Sondermann, F. H. Yildiz, The ins and outs of cyclic di-GMP signaling in *Vibrio cholerae*. *Curr. Opin. Microbiol.* **36**, 20–29 (2017).
47. L. Townsley, F. H. Yildiz, Temperature affects c-di-GMP signalling and biofilm formation in *Vibrio cholerae*. *Environ. Microbiol.* **17**, 4290–4305 (2015).
48. B. J. Koestler, C. M. Waters, Bile acids and bicarbonate inversely regulate intracellular cyclic di-GMP in *Vibrio cholerae*. *Infect. Immun.* **82**, 3002–3014 (2014).
49. R. A. Schaller, S. K. Ali, K. E. Klose, D. M. Kurtz Jr., A bacterial hemerythrin domain regulates the activity of a *Vibrio cholerae* diguanylate cyclase. *Biochemistry* **51**, 8563–8570 (2012).
50. A. Hsiao, Z. Liu, A. Joelsson, J. Zhu, *Vibrio cholerae* virulence regulator-coordinated evasion of host immunity. *Proc. Natl. Acad. Sci. U.S.A.* **103**, 14542–14547 (2006).
51. A. Hsiao, K. Toscano, J. Zhu, Post-transcriptional cross-talk between pro- and anti-colonization pili biosynthesis systems in *Vibrio cholerae*. *Mol. Microbiol.* **67**, 849–860 (2008).
52. C. Chun, L. Zheng, S. P. Colgan, Tissue metabolism and host-microbial interactions in the intestinal mucosa. *Free Radic. Biol. Med.* **105**, 86–92 (2017).
53. L. Zheng, C. J. Kelly, S. P. Colgan, Physiologic hypoxia and oxygen homeostasis in the healthy intestine. A review in the theme: Cellular responses to hypoxia. *Am. J. Physiol. Cell Physiol.* **309**, C350–C360 (2015).